Supporting Information

Unraveling the interfacial structure-performance correlation of flexible metal-organic framework membranes on polymeric substrates

Jingwei Hou,[a,b] Putu D. Sutrisna,[a] Tiesheng Wang,[b] Song Gao,[a] Qi Li,[c] Chao Zhou,[b] Shijing Sun,[d] Hao-Cheng Yang,[e] Fengxia Wei,[b] Michael T. Ruggiero,[f] J. Axel Zeitler,[g] Anthony K. Cheetham,[b] Kang Liang,[a,g] Vicki Chen[a,h,*]

[a]*School of Chemical Engineering, The University of New South Wales (Australia)*
[b]*Department of Materials Science and Metallurgy, The University of Cambridge (UK)*
[c]*Department of Chemical Engineering and Biotechnology, University of Cambridge (UK)*
[d]*Department of Mechanical Engineering, Massachusetts Institute of Technology, Cambridge MA (USA)*
[e]*Nanoscience & Technology Division, Argonne National Laboratory (USA)*
[f]*Department of Chemistry, University of Vermont (USA)*
[g]*Graduate School of Biomedical Engineering, The University of New South Wales (Australia)*
[h]*School of Chemical Engineering, University of Queensland (Australia)*

[*]Corresponding author:
Prof. Vicki Chen
Email: v.chen@uq.edu.au

Supporting text

ZIF-8 crystallization mechanism on membrane surface

Upon the mixing of metal ions and organic ligands, they can rapidly form poorly crystalline clusters in solution, possessing medium-range order related to van der Waals intermolecular interactions.[1,2] Their surface-coordinated neutral, nondeprotonated, positively charged 2-methylimidazole (Hmim) layer is in favour of interacting with polar solvent (*i.e.* water), preventing their attachment onto the positively charged PDA/PEI coated membrane surface. Therefore, no Bragg diffraction peak is observed at the early stage of ZIF-8 deposition (Fig. S5c-d).

Then due to the locally concentrated Zn ions by PDA on the membrane surface, the local consumption of excess Hmim can decrease the cluster surface charge, destabilize the colloids and facilitate their attachment onto the supporting membrane surface.[3] In addition, considering the pK_a value of chain PEI is around 8.2 to 9.5,[4,5] which is only slightly lower than $[Zn(Hmim)]^{2+}$ (10.3),[2] PEI on the membrane surface can also act as competitive Schiff base to deprotonate the bridging bidentate ligand on the clusters floating in solution, facilitating the transfer of clusters to highly crystalline structures with long range order at the membrane surface.[6,7] Similar cluster-crystal transformation processes are also observed in zeolite systems.[8] It should be noted that the MOF deposition process is complex and may be subject to the effect of different factors. In this work, the PDA-only modified PVDF results in an incoherent ZIF-8 layer (Fig. S4). The large number of catechol groups from PDA can effectively chelate a locally excessive amount of Zn ions, which would disrupt the nucleation of ZIF-8 on the membrane surface.[9,10] In comparison, for the PEI/PDA composite functionalized layer, catechol groups partially react with PEI chains via a Schiff-base reaction,[3] suppressing the undesirable effect of the PDA alone and leading to better ZIF-8 deposition and growth.

In terms of the contracted ZIF-8 structures, Venna et al. [6] synthesized ZIF-8 in methanol solution and reported a contraction of ZIF-8 structure at its early cluster stage, indicating the ZIF-8 structure at its metastable stage is susceptible to the external conditions. In their work, the contracted ZIF-8 then rapidly disappeared due to the Ostwald ripening process.[6] In comparison, in this work the immobilized metastable ZIF-8 may preserve their contracted structure at the interface, and may further affect the membrane performance and subsequent ZIF-8 growth.

It should be noted for the TiO_2 functionalized support, although it still has abundant –NH2 functional groups on its surface, its interaction with ZIF-8 is expected to be lower compared with the PDA/PEI supports, due to the presence of multiple interactions (-NH_2, π- π interactions and catechol groups) for the PDA/PEI supports.

Scheme S1. Schematic illustration of PDA/PEI membrane modification and ZIF-8 deposition processes. (a) Mechanism of PDA/PEI reaction and (b) scheme of membrane modification and ZIF-8 deposition.

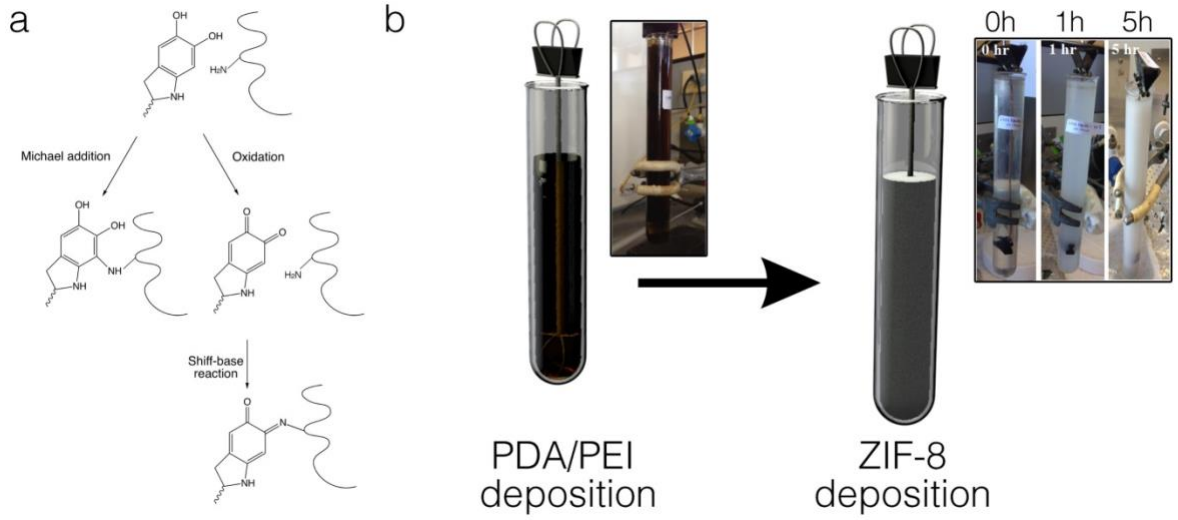

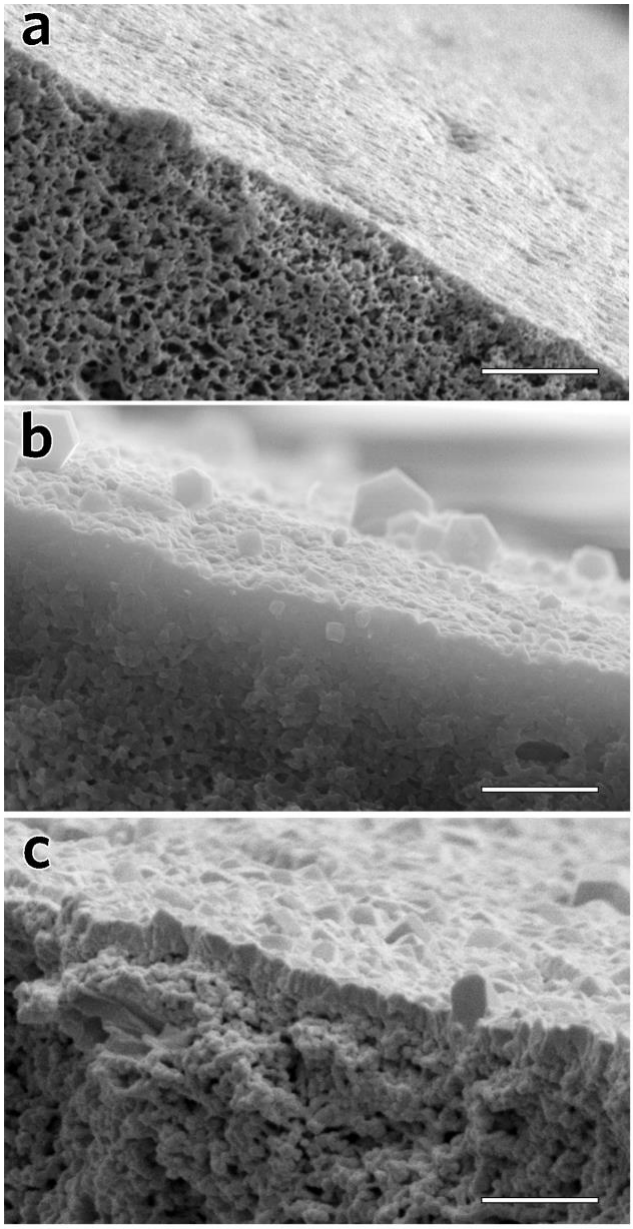

Fig. S1 Cross-sectional SEM image of (a) unmodified PVDF support, (b) ZIF-8 membrane with 5h deposition on PDA/PEI functionalized PVDF hollow fiber surface, and (c) ZIF-8 membrane with 5h deposition on TiO_2 functionalized PVDF hollow fiber surface. Scale bars are 2 μm.

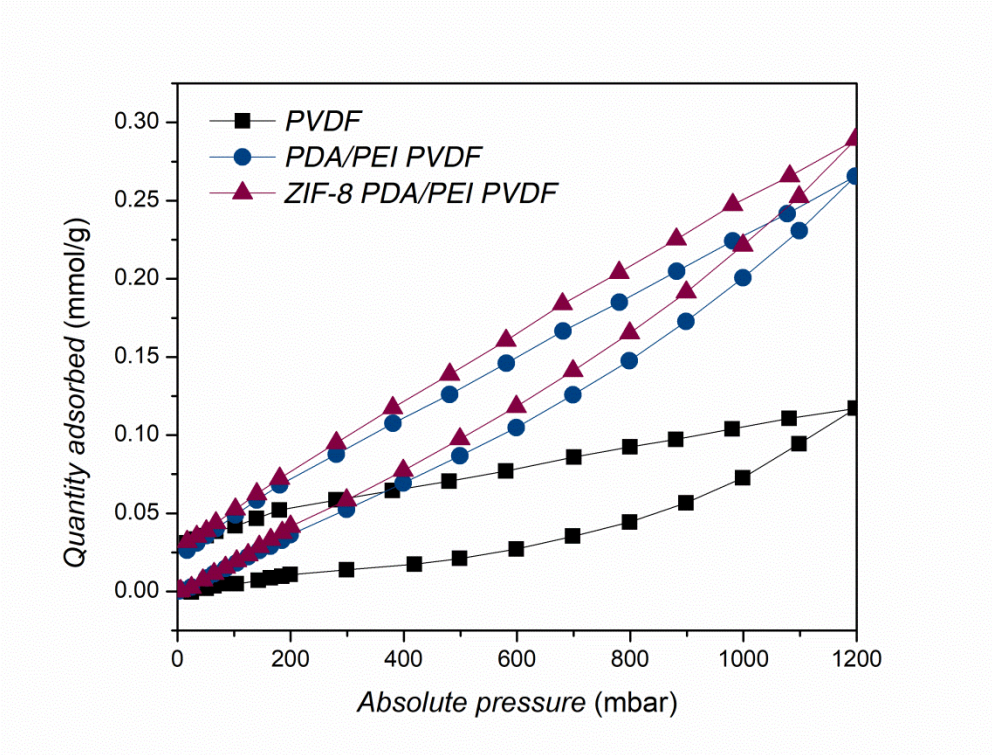

Fig. S2 CO_2 adsorption-desorption profile for different membranes. ZIF-8 membrane was fabricated with 5 h deposition on PDA/PEI PVDF supports.

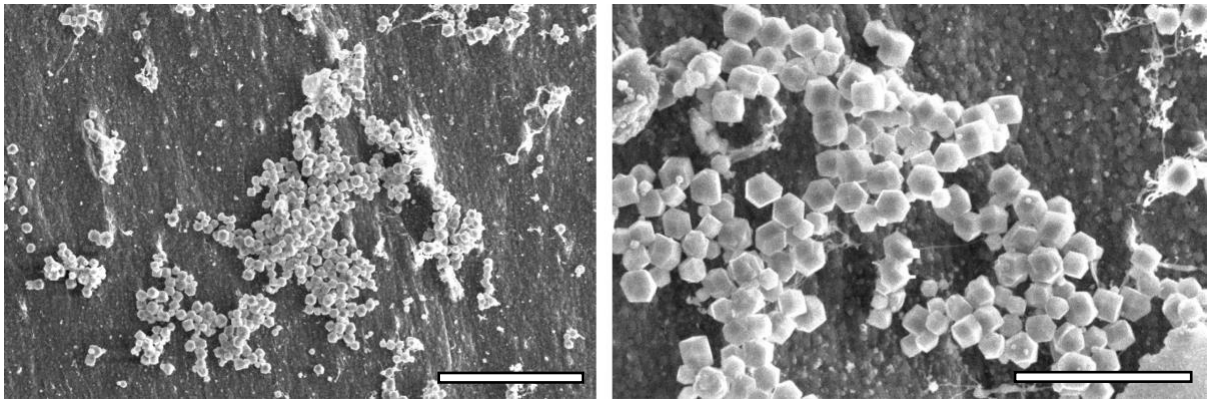

Fig. S3 SEM image of the ZIF-8 deposition on the unmodified PVDF surface. ZIF-8 deposition time was 5 h. Scale bars are 10 μm (left) and 5 μm (right).

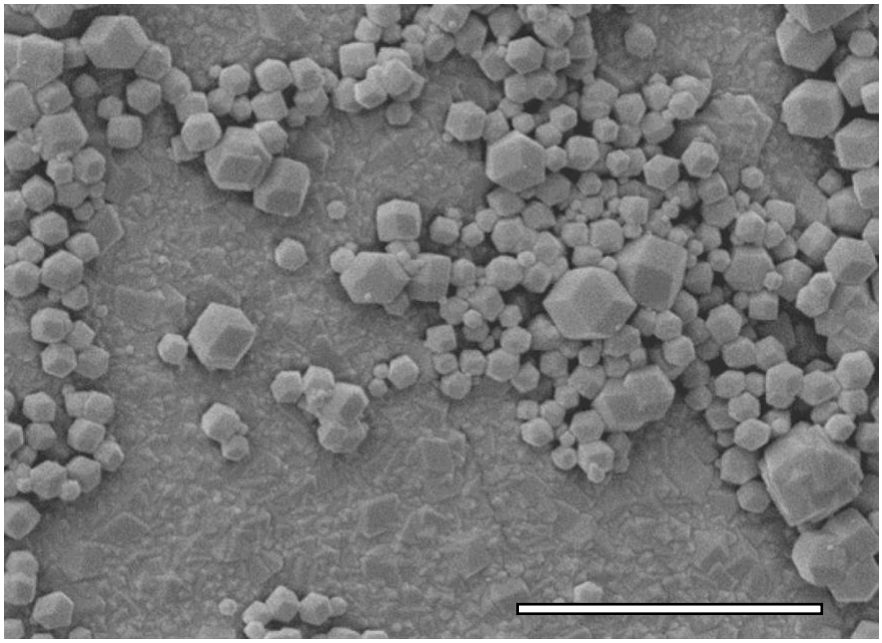

Fig. S4 SEM image of the ZIF-8 deposition on the PDA-only modified PVDF surface. Supporting PVDF was subject to 6 h PDA modification without the presence of PEI, and the ZIF-8 deposition time was 5 h. Scale bar is 5 μm.

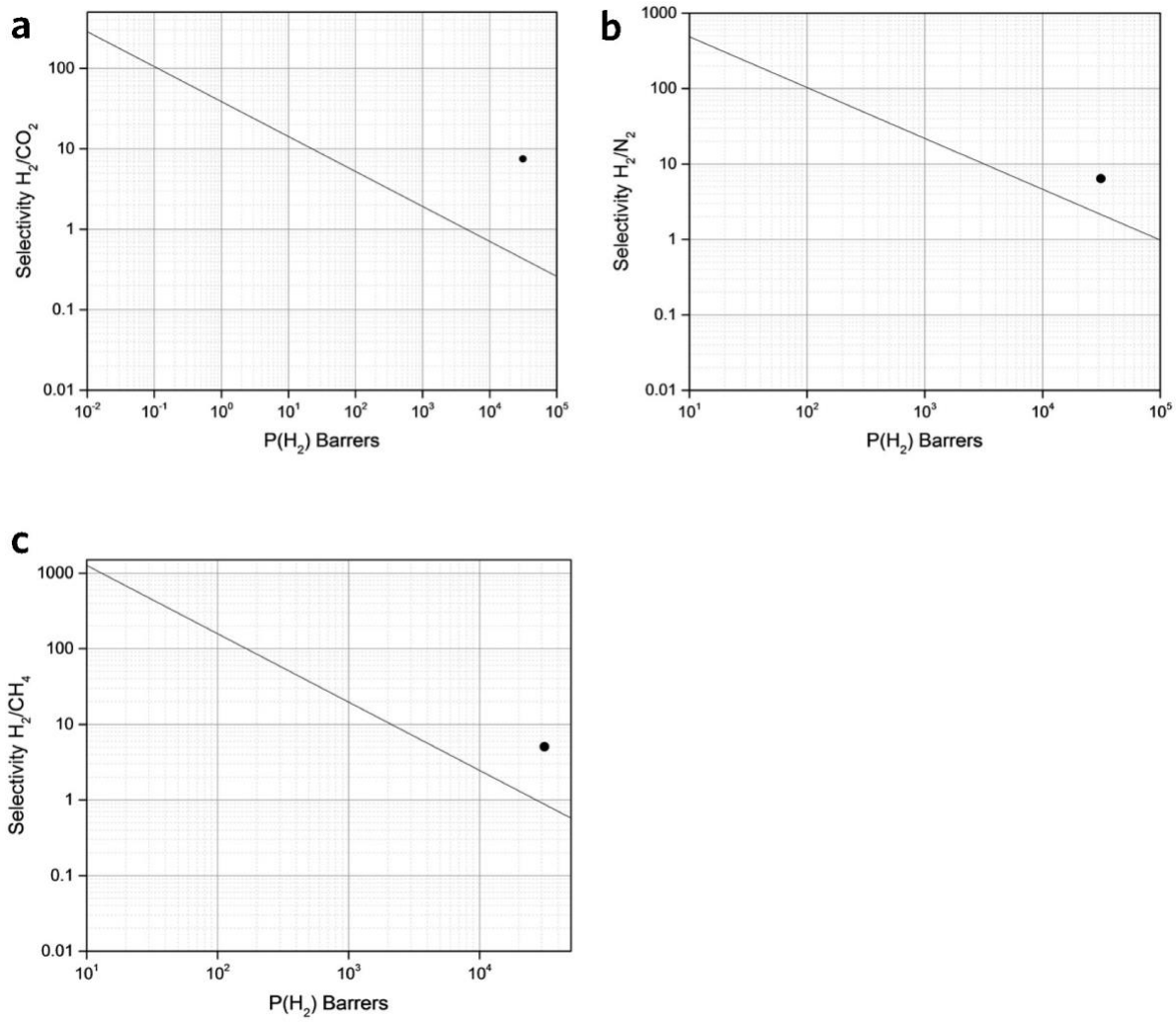

Fig. S5 Comparison of ZIF-8 membrane performance with Robeson plot: (a) H_2/CO_2, (b) H_2/N_2 and (c) H_2/CH_4 gas pairs.[11]

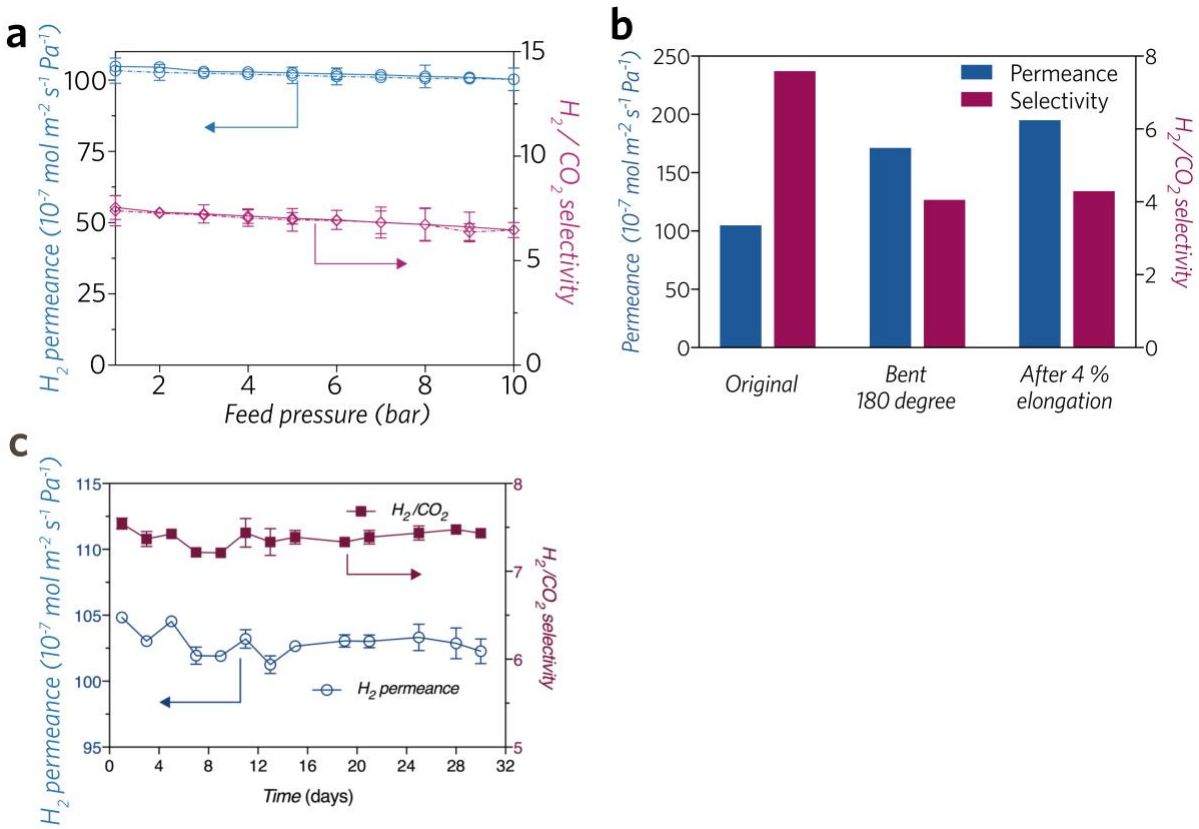

Fig. S6 Stability tests of the ZIF-8 membrane on PDA/PEI functionalized support. (a) Hydrogen permeance and H_2/CO_2 selectivity of the ZIF-8 membrane under different feed pressures. Solid line: pressurization and dash line: depressurization. b) Membrane performance after different mechanical stress. (c) Stability test of ZIF-8 membrane over 30 days operation.

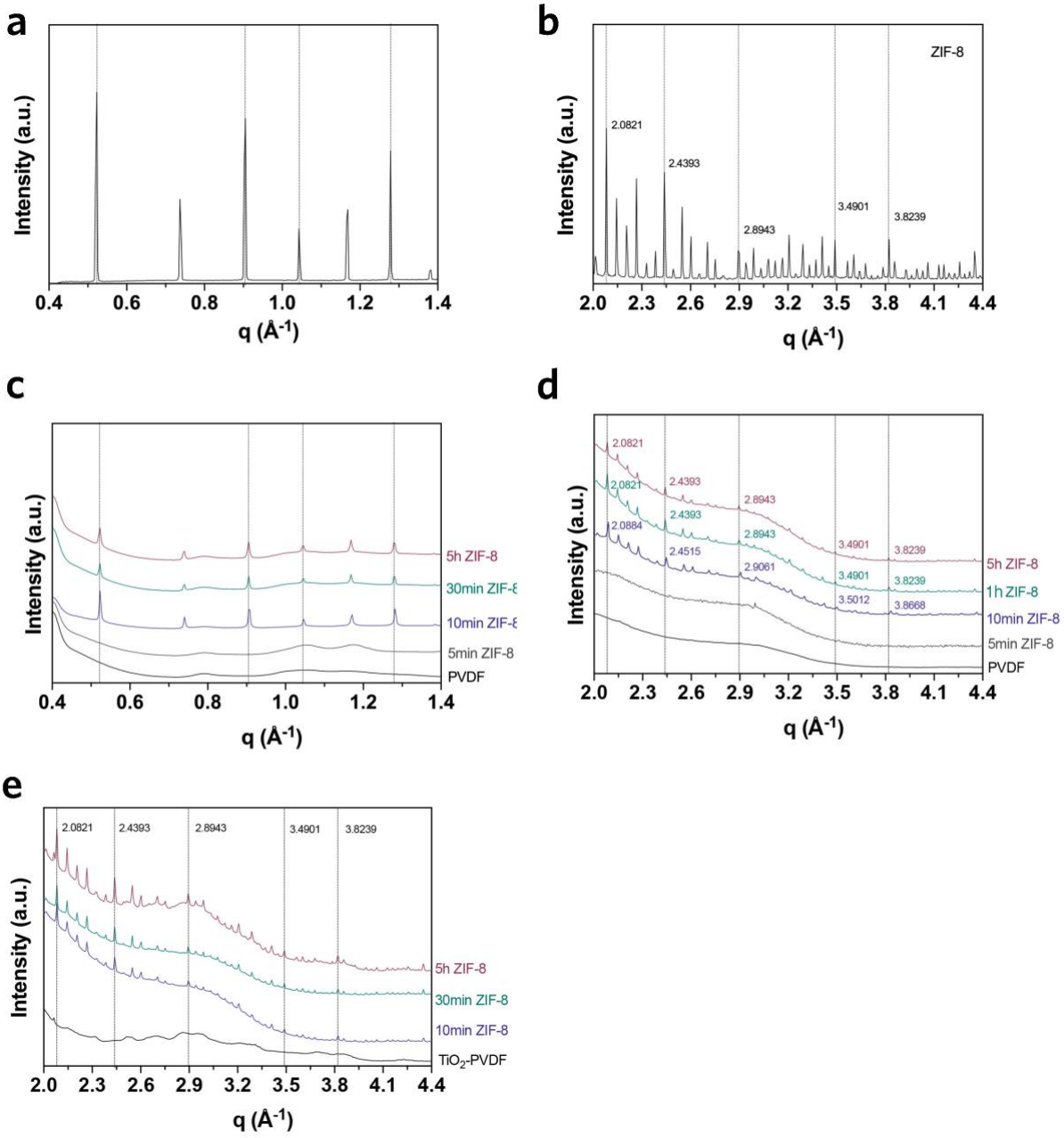

Fig. S7 SAXS (a) and WAXS (b) for benchmark reference ZIF-8 crystal powders. SAXS (c) and WAXS (d) for ZIF-8 deposited on PDA/PEI PVDF supports. WAXS (e) for ZIF-8 deposited on TiO_2 functionalized PVDF supports.

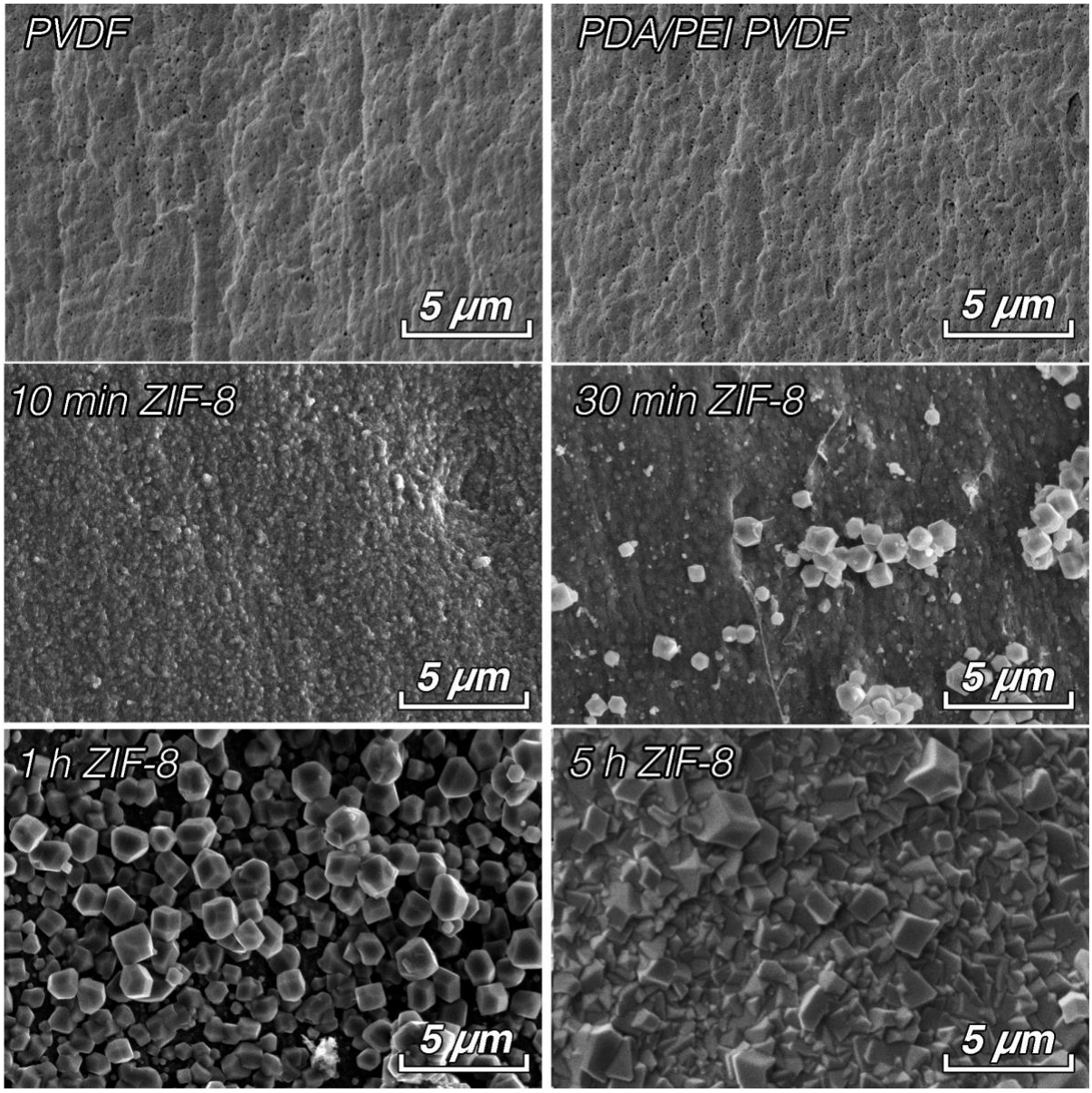

Fig. S8 SEM images of the ZIF-8 deposition process as a function of time on a PDA/PEI modified PVDF surface.

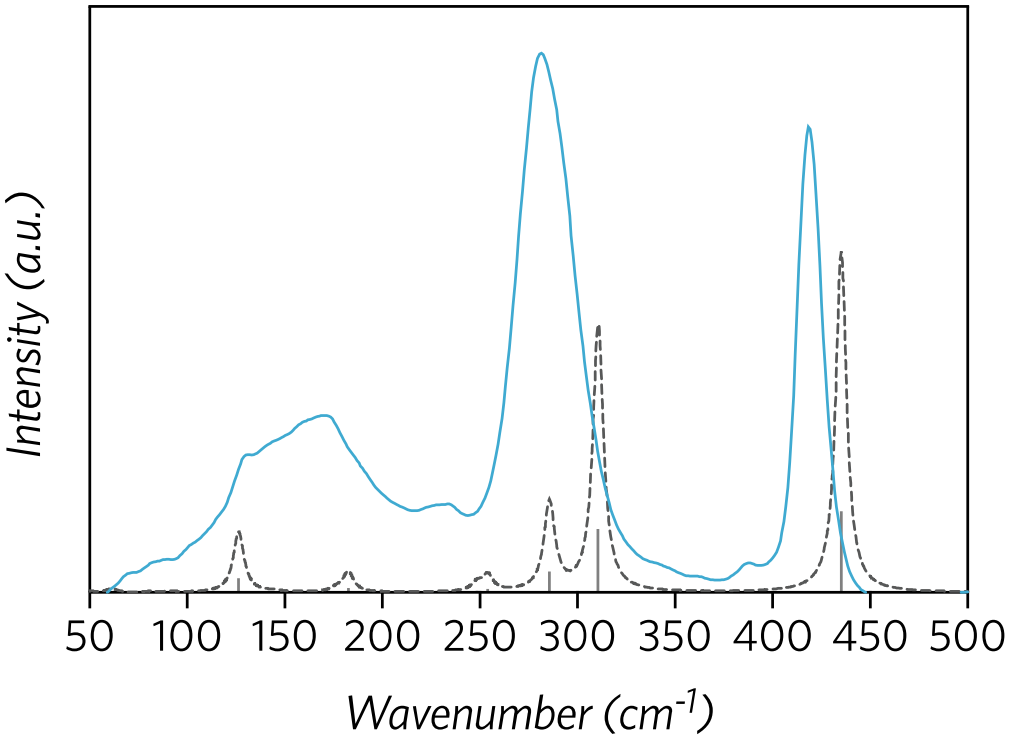

Fig. S9 Expermental low-frequency vibrational THz-FTIR spectrum of ZIF-8 seed layer on TiO_2 support (blue) as well as the simulated IR-spectra (black).

Table S1. Change of the average pore size of the hollow fiber PVDF after different treatments

Sample	Original PVDF	PVDF with 6 h PDA/PEI coating	PVDF with 12 h PDA/PEI coating	PVDF with functionalized TiO_2 coating
Average Pore Diameter (nm)	53.0 ± 3.4	44.5 ± 2.8	35.6 ± 6.8	45.7 ± 3.1

Table S2. Summary of membrane performance and comparison against our previous TiO_2 functionalized membrane.

	Gas permeance (10^{-7} mol m^{-2} s^{-1} Pa^{-1})				Gas selectivity				
	Pure H_2	Pure CO_2	Pure CH_4	Pure N_2	H_2/CO_2	H_2/N_2	H_2/CH_4	CO_2/N_2	CO_2/CH_4
Pure PVDF	707.3	173.9	282.9	219.1	4.1	3.2	2.5	0.79	0.61
PVDF - ZIF-8 (5 h)	522.2	126.7	195.0	151.7	4.1	3.4	2.7	0.84	0.65
PVDF - PDA (6 h)	578.8	137.0	216.9	163.7	4.2	3.5	2.7	0.84	0.63
PVDF - PDA (6 h) - ZIF-8 (5h)	569.4	104.8	159.3	119.6	5.4	4.8	3.6	0.88	0.66
PVDF - PDA/PEI (6 h)	668.2	153.4	297.1	186.6	4.4	3.6	2.3	0.82	0.52
PVDF - PDA/PEI (12 h)	456.0	104.2	174.4	128.3	4.4	3.6	2.6	0.81	0.60
PVDF - PDA/PEI (6 h)- ZIF-8 (1 h)	174.1	39.3	72.9	47.4	4.4	3.7	2.4	0.83	0.54
PVDF - PDA/PEI (6 h)- ZIF-8 (2 h)	167.6	33.5	60.4	41.9	5.0	4.0	2.8	0.80	0.55
PVDF - PDA/PEI (6 h)- ZIF-8 (3 h)	150.6	28.8	45.5	34.9	5.2	4.3	3.3	0.82	0.63
PVDF - PDA/PEI (6 h)- ZIF-8 (4 h)	117.2	19.2	30.2	23.3	6.1	5.0	3.9	0.83	0.64
PVDF - PDA/PEI (6 h)- ZIF-8 (5 h)	104.9	13.8	20.8	16.3	7.6	6.4	5.0	0.85	0.66
PVDF - PDA/PEI (6 h)- ZIF-8 (7 h)	96.7	12.9	19.1	15.5	7.4	6.2	5.1	0.84	0.68
PVDF - PDA/PEI (6 h)- ZIF-8 (9 h)	92.9	12.5	17.5	14.6	7.4	6.4	5.3	0.85	0.71
PVDF - TiO_2	556.1	121.8	199.0	150.5	4.6	3.6	2.8	0.81	0.61
PVDF - TiO_2 - ZIF-8 (5 h)	130.7	18.7	16.8	15.2	7.1	7.7	8.7	1.1	1.2

Table S3. Refinement results via Pawley method for ZIF-8 on different membrane supports. The diffraction pattern was converted from WAXS results, and 20-40 degree range was refined.

	Lattice parameters (Å)	Strain parameter (Voigt model)	Rwp%
ZIF-8 on PDA/PEI 10 min	17.029(6)	0.00038	1.09
ZIF-8 on PDA/PEI 5 h	17.083(2)	0.00061	0.98
ZIF-8 on TiO_2 10 min	17.077(0)	0.00008	1.32
ZIF-8 on TiO_2 5 h	17.081(8)	0.00081	2.33

Reference

(1) Cravillon, J.; Schröder, C. A.; Nayuk, R.; Gummel, J.; Huber, K.; Wiebcke, M. Fast Nucleation and Growth of ZIF-8 Nanocrystals Monitored by Time-Resolved *in situ* Small-Angle and Wide-Angle X-Ray Scattering. *Angew. Chem. Int. Ed.* **2011**, *50* (35), 8067–8071.

(2) Cravillon, J.; Nayuk, R.; Springer, S.; Feldhoff, A.; Huber, K.; Wiebcke, M. Controlling Zeolitic Imidazolate Framework Nano- and Microcrystal Formation: Insight into Crystal Growth by Time-Resolved *in situ* Static Light Scattering. *Chem. Mater.* **2011**, *23* (8), 2130–2141.

(3) Yang, H.-C.; Waldman, R. Z.; Wu, M.-B.; Hou, J.; Chen, L.; Darling, S. B.; Xu, Z.-K. Dopamine: Just the Right Medicine for Membranes. *Adv. Funct. Mater.* **2018**, *28* (8), 1705327.

(4) Ziebarth, J. D.; Wang, Y. Understanding the Protonation Behavior of Linear Polyethylenimine in Solutions through Monte Carlo Simulations. *Biomacromolecules* **2010**, *11* (1), 29–38.

(5) von Harpe, A.; Petersen, H.; Li, Y.; Kissel, T. Characterization of Commercially Available and Synthesized Polyethylenimines for Gene Delivery. *J. Controlled Release* **2000**, *69* (2), 309–322.

(6) Venna, S. R.; Jasinski, J. B.; Carreon, M. A. Structural Evolution of Zeolitic Imidazolate Framework-8. *J. Am. Chem. Soc.* **2010**, *132* (51), 18030–18033.

(7) Bux, H.; Feldhoff, A.; Cravillon, J.; Wiebcke, M.; Li, Y.-S.; Caro, J. Oriented Zeolitic Imidazolate Framework-8 Membrane with Sharp H_2/C_3H_8 Molecular Sieve Separation. *Chem. Mater.* **2011**, *23* (8), 2262–2269.

(8) Davis, M. E.; Lobo, R. F. Zeolite and Molecular Sieve Synthesis. *Chem. Mater.* **1992**, *4* (4), 756–768.

(9) Yao, J.; Dong, D.; Li, D.; He, L.; Xu, G.; Wang, H. Contra-Diffusion Synthesis of ZIF-8 Films on a Polymer Substrate. *Chem. Commun.* **2011**, *47* (9), 2559.

(10) Shi, Q.; Chen, Z.; Song, Z.; Li, J.; Dong, J. Synthesis of ZIF-8 and ZIF-67 by Steam-Assisted Conversion and an Investigation of Their Tribological Behaviors. *Angew. Chem. Int. Ed.* **2011**, *50* (3), 672–675.

(11) Robeson, L. M. The Upper Bound Revisited. *J. Membr. Sci.* **2008**, *320* (1–2), 390–400.